

SUGAR–1 Spectrometry in Ultraviolet of GALaxies at Redshift–1

Carlos Álvarez¹, Henrik H. Andersen², Luca Boschini³, André Burzlaff⁴, Michelle Conway⁵, Peter Laursen⁶, J. Miguel Mas-Hesse⁷, Jean-Luc Menut⁸, Nicole Nesvacil⁹, Linda Östman¹⁰, Cristina Rodríguez López¹¹, Demerese Salter¹², Ann-Marie Stobbart¹³, Guido van der Wolk¹⁴, Jean-François Vandenrijt¹⁵, Gordon Whitcomb¹⁶, and Andreas Zeh¹⁷

¹ Max-Planck Institut für Astronomie, Germany

² Astronomical Observatory. University of Copenhagen, Denmark

³ Alenia Spazio S.p.A., Laben, Italy

⁴ Fachhochschule Aachen, Germany

⁵ University College Dublin, Ireland

⁶ Astronomical Observatory. University of Copenhagen, Denmark

⁷ Centro de Astrobiología (CSIC-INTA), Spain

⁸ Observatoire de la Cote d'Azur, France

⁹ European Southern Observatory, Chile

Dept. of Astronomy. University of Vienna, Austria

¹⁰ Stockholm University, Sweden

¹¹ Universidad de Vigo, Vigo, Spain

¹² Leiden Observatory, The Netherlands

¹³ University of Leicester, UK

¹⁴ University of Groningen, The Netherlands

¹⁵ Centre Spatiale de Liege, Belgium

¹⁶ ESA

¹⁷ Thüringer Landessternwarte Tautenburg, Germany

Received September 00, 2004; accepted March 00, 2005

Abstract. This paper describes the outcome of the work performed during the 28th Alpbach Summer School *, focused on the theme *The Birth, Life and Death of Stars*. We propose a mission consisting of a large aperture (3.5 m main mirror diameter) UV space telescope, with capabilities for imaging and low, medium and high resolution spectroscopy. Even though such a telescope can have multiple scientific applications, we suggest a survey-type mission (SUGAR-1), dedicated mainly to the spectroscopic study of starburst galaxies at redshift $z \sim 1$, which corresponds to an epoch of enhanced star formation density in the history of the Universe and, in particular, to the time when our Solar System was born.

Key words. Space Telescope – Ultraviolet – Starburst Galaxies

1. Introduction

The present paper describes the work performed during the 28th Alpbach Summer School, held in the typical Tyrolean village of Alpbach between July 26 and August 6, 2004. During the School, European graduates, post-graduate students, young scientists and engineers are given the opportunity to expand and strengthen their knowledge of selected space issues in workshops which are part of the Summer School programme.

Send offprint requests to: Carlos Álvarez

* The Alpbach Summer School is organized by the Austrian Space Agency together with the Austrian Federal Ministry of Transport, Innovation and Technology, the European Space Agency and the national space authorities of all ESA member states.

This year, the School was focused on the theme *The Birth, Life and Death of Stars*.

Previous to the arrival at Alpbach, the School participants are distributed in 4 teams of approximately 15 members. Once there, resources are given to the teams (supervision by tutors, computing facilities and access to specialized bibliography), to face a challenge which, this year, consisted of designing a space mission to solve a *stellar mystery*. A friendly competition is set between the teams to stimulate the team work. The time is normally divided in lectures during the morning and workshops in the evening. The lectures are given by experts in the School theme, so that in our case, we could learn all about the organisational, scientific and technical aspects needed to define a space mission.

The workshops are the soul of the Summer School, where the students are given the opportunity to apply what was learnt during the lectures to their project. At the end of the two weeks, the teams must present a brief report of their work and there is a public presentation of the projects to a committee of experts. We were one of these teams, and what is presented below is an extract of our work during the Summer School.

1.1. The team

Institutions from 11 ESA member states were represented in our team, and similar distribution of nationalities was present in the other 3 teams. Our team members have different backgrounds in several fields of astronomy as well as engineering, with our academic formation ranging from undergraduate students to post-docs. Carlos Álvarez is a post-doc in observational IR astronomy, Henrik H. Andersen is doing his masters in scaling relations of galaxy clusters and the Sunyaev Zel'dovich effect, Luca Boschini is an electronic engineer and works as an electronic designer, André Burzlaff is studying astronautical engineering, Michelle Conway is a PhD student, Peter Laursen is a master student, Jean-Luc Menut is doing a PhD on modelling dust envelopes around evolved stars and signal analysis of the interferometric instrument APreS-MIDI, Nicole Nesvacil is a PhD student in astronomy, Linda Östman is a PhD student, Cristina Rodríguez López is a PhD student in photometry and spectroscopy of pre-white dwarfs, Demerese Salter is a master student, Ann-Marie Stobbart is studying X-Ray astronomy, Guido van der Wolk is a master student in astronomy and philosophy of science, Jean-Francois Vandenrijt is studying engineering and Andreas Zeh a PhD student in astronomy. Our main tutors were J. Miguel Mas-Hesse, who is an experienced scientist in the field of UV astronomy and Gordon Whitcomb, with many years of experience in managing space projects.

1.2. The experience during the School

As a team, the first and rather difficult task presented to us was that of deciding which *stellar mystery* we wanted to solve. It may look trivial from the outside, but from the inside, it took a good of two days of intense and fruitful discussions until we came to a decision. Basic points like the type of stellar phenomenon we wished to study, the wavelength range in which we wanted to operate or which observational technique we wanted to utilize were not easy to determine, when looked at them in detail. This was only the beginning and it was already fun!

Once we had defined our main science goal (spectrometry in the UV of galaxies at redshift-1), we faced the decision of selecting amongst us a team leader, which would serve as the team co-ordinator as well as the official contact with our tutors. This decision was rather straightforward, since during our previous discussions it was clear that Ann-Marie, our team leader elected by *consensus*, had a really good aptitude and attitude to communicate and to organize people. We then organized ourselves in two sub-teams, one focused on the science

aspects and the other on the technical aspects of the mission. Ann-Marie, Henrik, Michelle, Peter, Nicole, Linda and Cristina conformed the science team. Carlos, Luca, André, Jean-Luc, Demerese, Guido, Jean-Francois and Andreas conformed the technical team. We scheduled regular meetings between the sub-teams to communicate our findings to each other. This soon turned into a iterative process where the findings of one sub-team implied changes in the work performed by the other sub-team, and *vice versa*. Close to the submission and presentation of the project, everyone who had some spare time or had finished their assigned tasks was helping in any part of the project where a hand was needed, whether science or technical.

The last days of the School, and particularly the last night, were of very intense work. The atmosphere in the working room during the last night was very special. All four teams had by then defined their projects and it was the time of *giving the rest* to prepare the report and the presentation. In our case, Ann-Marie was carrying most of the weight of the report preparation and Jean-Francois was in charge of preparing the presentation, but we all were there working to finish the job on time. Finally and after a long but intense night, four of our team members (Ann-Marie, Henrik, Jean-Francois and André), where still fresh enough to give the final presentation to the committee of experts. After their presentation, the whole team was answering the questions of the committee about specific parts of the project.

The work we did would not had been possible without the supervision of our tutors. They were available 24 hours a day to solve any problem and to answer any question we had. They were also helping to guide the project in the right direction, and would advise on how much stress should be given and time should be spent on each aspect of our space mission design. Even though each team had officially one tutor and there were several *roving* tutors available for all teams, in practice all tutors were advising all teams, which favored the nice atmosphere that was felt during the School.

In a similar way as the tutors, the lectures and the lecturers were fundamental pieces during the preparation of the projects. Lectures were a continuous source of ideas and lecturers were available at any time to be asked questions or for advise related to the mission preparation.

Even though a large fraction of our time in Alpbach was spent working on our project, there was also enough time to do other activities. Every day, we had evening dinners, where all students tutors and lecturers were brought together at the same table, chatting, watching slide shows, singing, telling jokes or listening to evening lectures on borderline astronomical topics. The School organisation also prepared weekend activities like a day out hiking in the mountains and a visit to a planetarium. We all had the opportunity to enjoy the beauty of the Austrian Tyrol and to experience the hospitality of the people from Alpbach.

1.3. The lessons learnt

For many of us this was the first contact with the world of scientific space research and with the problems related to it. One lesson we learnt during our participation in the Alpbach Summer

School was to work as a team with a determined amount of resources in a limited amount of time to achieve a specific goal, in our case a mission design. During the process, we realized that it is not possible to design a space mission if there is not communication between the scientists, who are focused on the specific problems to solve, and the engineers, who in the end will materialize the project.

We also learnt to work in an international environment. It was extraordinary to experience how in a matter of hours, a group of 15 people that had never met each other before, managed to evolve to a situation of highly intellectual interaction to define and solve a problem. Each of us had to do a balancing exercise between keeping individual views and also accepting other member's opinions to ensure the team to work smoothly and efficiently. We soon learnt which was each team member's expertise, and in the case of doubt who was the person to ask for advise. Another interesting aspect of the School is the fact that most of us were performing tasks that were not directly related to our background. In other words, the School conformed a fantastic opportunity to learn about concepts differing from those we commonly use in our studies of jobs.

We had to face several problems and difficulties that appeared during the design process. Perhaps, one of the most difficult to deal with was the School timescale. Everything had to be assimilated very fast and decisions had to be made very quickly. We all had the impression in the end that we could have done a much better job if we had had more time. However these were the rules of the game and we all had accepted them. Besides, we are satisfied with our achievements having in mind the mentioned time restrictions.

In summary, during the School we learnt to improve our personal relations. At the end of this experience we were not just a group of students but a team of friends! We are still in contact and are planning to meet again for holidays. And of course, we made friends not only within our team, but also with members of other teams, since the competition aspect of the School was obviously not taken too seriously. If one of the Alpbach Summer School aims is to favour relations between collaborators of scientific institutes and universities from all over Europe, the aim was perfectly accomplished this time.

2. Science case

Stars are the fundamental building blocks of galaxies. A major aspect of understanding galaxy formation and evolution is to understand their star formation history. Starburst galaxies are galaxies experiencing intense star forming activity and exhibiting strong UV emission from a young, hot stellar population (see Fig. 1). The study of starbursts helps us to understand the star formation process, and its influence on the environment and processes in the interstellar gas. The study of the star formation rate (SFR) at various redshifts is possible from the intensities of the $H\alpha$, $H\beta$, $O II$ and $O III$ lines, and the luminosity of the UV continuum. These can be used to generate Madau plots (Lilly et al. 1996; Madau et al. 1996; Rosa-González et al. 2002; see Fig. 2) which represent the SFR-density as a function of the redshift z .

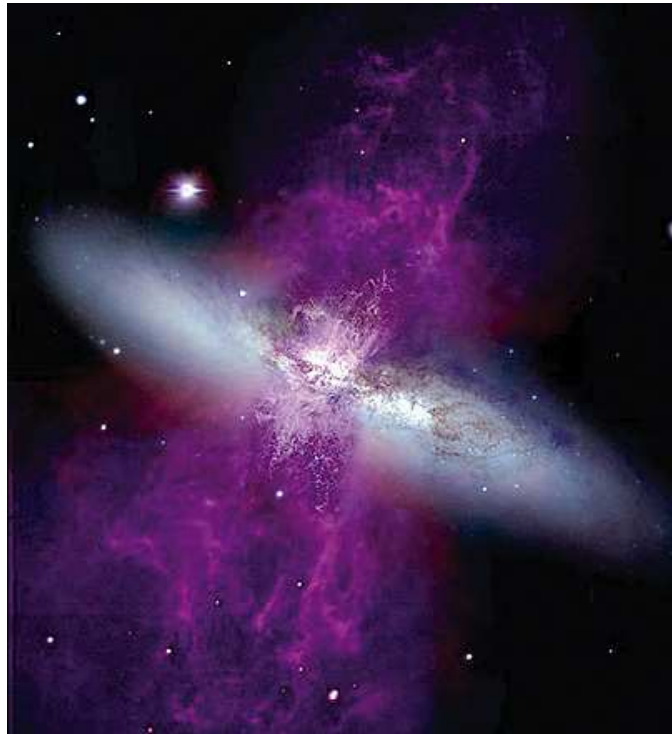


Fig. 1. This image is a color-coded picture of the archetypal starburst galaxy M82. It shows the horizontal stellar disk of the galaxy, which harbors its active star formation, and a perpendicular supergalactic wind of ionized gas powered by the energy released in the starburst. Purple represents emission in ionized hydrogen ($H\alpha$) and ionized nitrogen, and the green is ionized sulfur. Adopted from Mark Westmoquette (University College London), Jay Gallagher (University of Wisconsin-Madison), Linda Smith (University College London), WIYN/NSF, NASA/ESA

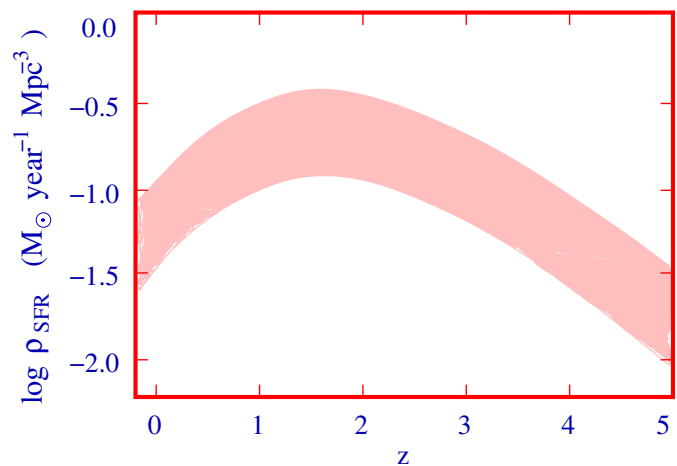


Fig. 2. Sketch of a Madau Plot, where the density of star formation rate is represented for different redshifts. The pink band indicates the star formation history of the Universe. A peak can be appreciated at $z \sim 1$, which corresponds in time with the birth of our Solar System.

Madau plots indicate that a peak of star formation in the history of the Universe occurred at $z \sim 1$, which corresponds to ~ 5 Gyr, i.e. the epoch of the birth of our own Solar System. Observations of this era will enable us to investigate the initial conditions in galaxies like ours when the Solar System forma-

tion was triggered. By observing a large number of galaxies at $0.4 < z < 1.1$, we can learn about the properties of the star formation processes and the conditions of the interstellar medium (ISM) and its chemical properties at this moment of enhanced star formation. Spectroscopy and imaging in the UV will have a great impact on galaxy evolution modelling, since they will provide insight on whether the time corresponding to $z \sim 1$ was a time of massive galaxy formation, or if the massive star formation of that time took place in already established galaxies, which were formed at a much earlier stage in the evolution of the Universe. Moreover, studies of the Universe at $z \sim 1$ are of cosmological relevance, because according to the Cosmological Standard Model, it is precisely at $z \sim 1$ when the Universe underwent a phase transition from matter density Ω_{Matter} being larger than dark energy density $\Omega_{\text{DarkEnergy}}$, to the opposite.

Therefore, to investigate this interesting time in the evolution of the Universe, we suggest the construction of a dedicated UV telescope with a pre-defined science mission to perform Spectrometry in Ultraviolet GALaxies at Redshift-1 (SUGAR-1). In what follows, a more detailed description of the mission science goals is given (Section 3). In Section 4, we show how the science goals are transformed into science requirements for the mission, which are, in Section 5, turned into telescope and instrument requirements. In Section 6, a brief description is given of the main technical aspects of the mission (spacecraft structure, electronics, power and orbit). The spacecraft mass and cost budgets of the mission are addressed in Section 7, ending with a final summary (Section 8).

3. Science goals

The proposed UV telescope would allow to completely characterize the properties of the star formation episodes that took place at around $z \sim 1$. In this section we specify the different parameters that could be analyzed with this mission.

3.1. Star formation process

3.1.1. Initial Mass Function

An important aspect of studying the properties of galaxies is the Initial Mass Function (IMF), i.e. the function that describes the distribution of stars of different masses. An essential goal of our project is to derive the IMF of a large sample of galaxies around $z \sim 1$, which will provide insight on the so far poorly known process of star formation in this era. The IMF can be determined by comparing some observable parameters with the predictions of evolutionary synthesis models. According to (Cerviño & Mas-Hesse 1994) (hereafter CMH94), the combination of the two strong metal absorption lines Si IV (λ 1400 Å) and C IV (λ 1550 Å) formed in the atmospheres of massive stars, together with the H β emission line equivalent width, allow to constrain simultaneously both the slope of the IMF and the age of the young massive stellar cluster.

While the Si IV and C IV themselves depend strongly on metallicity Z , the ratio of their equivalent widths $W(\text{Si IV})/W(\text{C IV})$ appears to be essentially insensitive to it

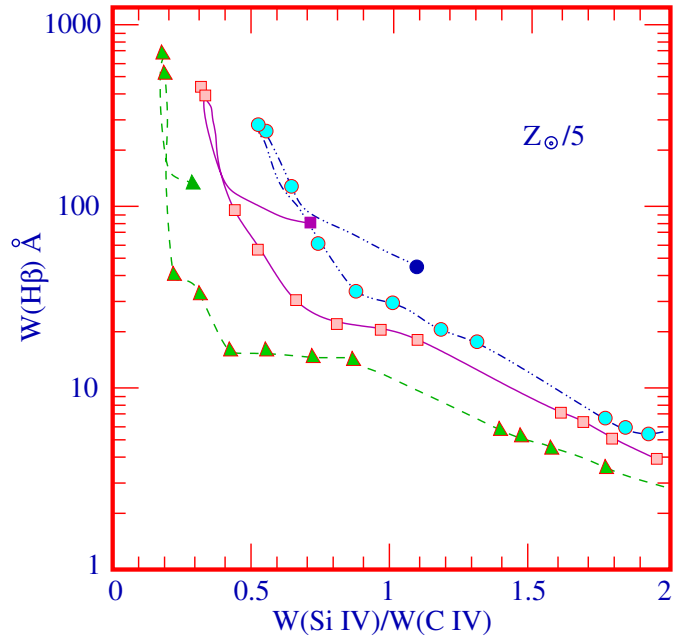


Fig. 3. This figure, adopted from CMH94, shows the relationship between $W(\text{H}\beta)$ and the ratio $W(\text{Si IV})/W(\text{C IV})$ for a metallicity 5 times lower than the solar metallicity (Z_{\odot}) and 3 different IMF slopes. CMH94 show similar trends for metallicities in the range from Z_{\odot} to $Z_{\odot}/20$. Each sequence correspond to a given value of the IMF slope, with the central one being the standard Salpeter IMF. The symbols have been plotted at intervals of 1 Myr, starting from an age of 1 Myr at the upper left. The short sequences at the top correspond to the predictions of extended star formation episodes, i.e., those producing stars at a constant rate during more than 20 Myr.

CMH94). Nevertheless, the evolution of the stars themselves depend on their intrinsic metallicities. We show in Fig. 3 the diagnostic diagram produced by CMH94. It can be seen that if both $W(\text{Si IV})/W(\text{C IV})$ and $W(\text{H}\beta)$ are measured, the diagram allows to determine uniquely both the slope of the IMF, and the evolutionary state of the starburst.

Since these diagnostic diagrams are dependent on metallicity, it would be needed to previously derive the metal abundances of the objects under study. This can be achieved by measuring the equivalent width of different metal absorption lines in the ISM. While the lines from the stars in the starburst region are broad and asymmetric, the lines from the surrounding interstellar medium will be narrow and thus easy to distinguish and measure. At $z \sim 1$, the wavelength of the H β and OIII emission lines will be in the Near-IR, and hence observable from ground. An independent measurement of the abundance will be therefore possible by using standard instrumentation and procedures.

3.1.2. Age and star formation regime

Fig. 4 shows the evolution of the H β equivalent width for different metallicities and for instantaneous (IB) and extended bursts (EB). In the Local Universe, it is known that massive star formation is happening more or less instantaneously. But for galaxies at $z \sim 1$, it is yet unclear if an instantaneous (lasting a

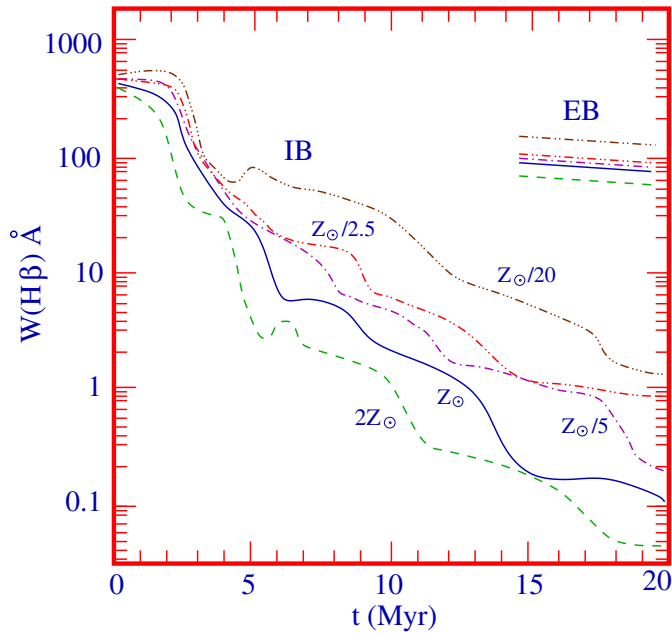


Fig. 4. Relationship between $W(\text{H}\beta)$ and age for different metallicities in the case of instantaneous (IB) and extended starburst (EB). Plots like this can be used to determine the age of a starburst, once the metallicity is known (adopted from CMH94).

few Myr) or an extended (> 20 Myr) star formation took place. In the case of nearly instantaneous bursts, the ionizing power decreases very rapidly, and so does $W(\text{H}\beta)$, while for extended episodes $W(\text{H}\beta)$ remains stable at around 100 \AA . Combining the measurements of this parameter with other ones, like the equivalent width of the lines associated to Wolf-Rayet stars, it is possible to also constrain the star formation regime, and to improve the estimates of the age achieved with the diagnostic diagrams.

3.1.3. History of star formation

The availability of ground-based optical observations will allow us to determine whether there are evolved stellar populations underlying the presently investigated young one. The continuum of an older population of the galaxy formed, for instance, in a starburst preceding the present one, would dominate the starburst in the optical, whereas the present starburst would dominate in the UV. The composite spectrum of the two populations can be derived from a combination of UV space-observations with the optical spectra obtained by ground-based surveys of galaxies. From the composite spectrum, it will be possible to conclude whether the starburst galaxy was formed at an earlier time or, if no underlying evolved population is detected, the galaxy is newly formed. It will also be possible to derive the relative starburst strength, i.e. the ratio of the mass transformed into stars by the current starburst to the total galaxy mass.

3.2. Massive Super Stellar Clusters

It is expected that the intense star formation episodes taking place in these galaxies will form a number of the so-called Super Stellar Clusters (SSCs), containing each more than $10^5 M_{\odot}$ in stars. Our proposed observations and analysis will allow to characterize the properties of the massive stars constituting these clusters, as well as their impact on the surrounding medium.

3.2.1. Effective temperature

The effective temperature T_{eff} of the cluster is defined as the temperature of a standard star which emits the same fraction of ionizing photons with energy above and below the helium ionization limit ($\lambda_{\text{rest}} = 504 \text{ \AA}$) as the whole region (CMH94). It is therefore a measure of the slope of the ionizing flux (Mas-Hesse & Kunth 1991). Using the model for the relation between T_{eff} , age, Z and the IMF, proposed in CMH94, the effective temperature of the SSC can be derived, and so its ionizing properties.

3.2.2. Dynamics of atmospheres

The OB-stars in the massive SSCs will, in general, exhibit high speed stellar winds. A fraction of the photons produced by the stars will therefore be absorbed in the winds moving towards us and emitted again at a slightly lower redshift. The resulting P Cygni line profile provides a direct measurement of the difference in speed between the star and the wind and is thus a measure of the terminal velocity of the latter. The UV lines of C IV and Si IV are formed in the wind component of the OB-stars and are strongly related to the cluster metallicity. Therefore, they are ideal diagnostic features for a dynamical study of starburst clusters.

3.3. Dynamics of surrounding gas

The dynamics of the surrounding gas will be affected by the release of mechanical energy by the newly formed stars, in the form of winds and supernova explosions. The supernova-rate (SNR) of a massive cluster can be estimated using the relationship between Z , IMF and age. With a given SNR, the amount of metals ejected into the surrounding sphere or into the intergalactic medium (IGM) can be estimated, as well as the total amount of mechanical energy.

In a similar way as metallic lines can be used for study of the cluster atmospheres, the $\text{Ly}\alpha$ line profile can be used to probe the dynamics of the gas surrounding the cluster. This will help to put constraints on the star formation history, e.g. allowing to estimate the total amount of kinetic energy released in the starburst. Additionally, the equivalent width, or in the case of saturation, the $\text{Ly}\alpha$ profile, can be used to measure the column density of neutral hydrogen along the line of sight.

3.4. Leaking of photoionizing photons into the IGM

At wavelengths below the Lyman-break ($\lambda < 912 \text{ \AA}$), the high energy photons created in a star forming region are usually absorbed by the H I atoms of the surrounding hydrogen cloud. Hence, below the Lyman-break, no UV flux would be detected from a star forming region shrouded by a density-bound cloud. If, however, the cloud is ionization-bound, photoionizing photons could be leaking through to the IGM. If this leaking photon flux is measurable, the intergalactic density of photoionizing photons could be estimated for $z \sim 1$. This knowledge could be further used for the analysis of the properties of intergalactic hydrogen clouds (IGCs). In our local universe ($z = 0$) these clouds are neutral, whereas at redshifts of $z \sim 10$ it is suspected that all hydrogen clouds are completely ionized. To determine the chemical composition of the IGCs, which would serve as a tool to distinguish between primordial clouds or clouds consisting of material ejected by galaxies, the fraction of ionization of the cloud must be known.

The fraction of escaping photons has been estimated by Heckman et al. (2001) to be $f_{\text{esc}} \leq 6\%$. A more realistic estimate depends on galactic parameters, such as the distribution of neutral hydrogen along the line of sight. The limit can be lowered further, if the dust extinction is accounted for.

The measurement of the photon leakage in a large number of galaxies at $z \sim 1$ can be used to estimate the ionization state of the intergalactic clouds at this epoch. Universe. If the leaking fraction is large enough, a significant fraction of the intergalactic cloud should be still ionized at this time.

3.5. Analysis of the extinction law

It is known that the *standard* extinction law differs not only from region to region within the Milky Way, but also from galaxy to galaxy. From the extinction law in a galaxy it is possible to derive the chemical composition and physical properties of its dust grains. It is therefore of interest to analyze the properties of the extinction law in many other non-local galaxies.

Evolutionary synthesis models show that the UV continuum slope is only slightly sensitive to parameters like age or Z during the first 10 Myr of evolution (especially if compared to the interstellar extinction effect). Therefore, comparing the observed UV continuum with the predicted one it is possible to derive the properties of the extinction law in these objects, and from here the properties of the interstellar dust particles.

3.6. Additional science

In addition to the main science goals described above, much more scientific research can be done with the UV mission proposed in this work. Some of the more interesting topics are,

- Imaging of nearby starburst galaxies and comparison with optical images.
- Investigation of the properties of the IGCs from the Ly α lines.
- Determining deuterium abundances in nearby stellar objects.

Table 1. Rest wavelength of the relevant spectral features.

Line	Wavelength (Å)
Lyman break	912
Si III	1261
Lyman α	1216
Si II	1260
O I	1302
C IV	1335
Si IV	1394,1403
Si II	1527
C IV	1548,1551

- High-resolution UV-spectroscopy of the hottest white dwarfs ($5 - 17 \times 10^4 \text{ K}$).

4. Science requirements

The first step to investigate the wide range of phenomena related to massive star formation at $z \sim 1$ described in the previous section, is to obtain a statistically significant list of galaxy candidates at $z \sim 1$, which should be selected from ground-based surveys. This will be available in a near future, once the Sloan Digital Sky Survey (SDSS) is completed, providing a wealth of starbursts to study in the UV at the required redshifts. Once a large number of candidates are available, we suggest a science mission consisting of two steps. Firstly, due to the long integration times required by the high spectral resolution observations (necessary to perform the line-profile studies), a space-based, low resolution survey of galaxies in the UV domain for $0.4 < z < 1.1$ will be carried out and interesting objects (mainly potential starburst galaxies) will be identified. In a second step, individual starbursts candidates will be observed in a high spectral resolution mode.

The major science topics to be addressed within the SUGAR-1 mission (Section 3) are translated into the following specific science requirements:

- *Wavelength range.* The wavelength coverage should be $1200 \text{ \AA} - 3500 \text{ \AA}$, to cover the Lyman break and at least the C IV absorption lines for all galaxies with $0.4 < z < 1.1$, enabling spectroscopic analysis of stellar and interstellar absorption features of individual starburst galaxies (see Table 1 for the rest wavelengths of the relevant spectral features). The lower limit will allow detecting the leaking photoionizing photons below the Lyman break.
- *Spectral resolution.* Spectral resolutions of $R = 500, 1000, 10000$ are needed for the continuum, to detect the ISM metal lines and stellar absorption lines, and to resolve the P Cygni profile of the Ly α line.
- *Sensitivity.* To work out the required sensitivity, we used the synthesis models for galaxies with active star formation, *Starburst 99* (Leitherer et al. 1999). The models predict that for a typical starburst galaxy transforming at least $10^8 M_{\odot}$ into stars and an age of 4 Myr, the limiting flux will be $2.5 \times 10^{-20} \text{ W m}^{-2} \text{ \AA}^{-1}$. A starburst galaxy at $z \sim 1$, with a young stars mass of $M > 10^5 - 10^6 M_{\odot}$ has a photon flux

Table 2. Main telescope parameters.

Element	Value
Effec. focal length	70 m
Primary mirror diam.	3.5 m
Secondary mirror diam.	0.3 m
F-ratio	f/20
Mirror materials	Graphite fibre composite
Reflecting surface	Al coating, protected with MgF ₂
Active optics	Carbon fibre structure 481 actuators 6 nm RMS res.

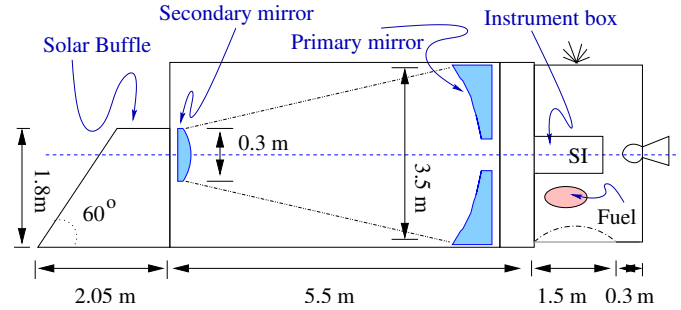
- in the ionizing UV of $F \geq 10^{52}$ photons s^{-1} . If $f_{esc} \sim 1\%$, the minimum flux reaching the Earth will be 10^{-22} W m^{-2} .
- *Signal/Noise (S/N)*: A S/N > 5 is needed for the detection of potential photon leakage at the Lyman break. A S/N > 10 is required to detect the Ly α line and study its profile, and a value > 20 is needed for metallic lines, which are relatively weak.
 - *Field of view (FOV)*: Starburst galaxies at $z \sim 1$ have a typical angular diameter of a few arcseconds, therefore a FOV of 30'' will suffice.

5. Telescope and instrument requirements

The science requirements described above yield the main constraints on the parameters defining the telescope and instrumentation planned on board the spacecraft. Our aim is to design a mission that allows surveying a large number of galaxies at $z \sim 1$ within the spectral range, sensitivity and S/N given in Section 4. Hence, a large collecting area and a large sensitivity will be mandatory to optimize the exposure times as much as possible.

For a $10^8 M_{\odot}$ starburst galaxy at $z = 1$ and a typical extinction ratio of 5, the *Starburst 99* models yield a flux density of $\sim 5.12 \times 10^{-21}$ W $m^{-2} \text{ \AA}^{-1}$. This will turn into a power of $\sim 4.9 \times 10^{-20}$ W \AA^{-1} at the surface of a 3.5 m diameter mirror. This corresponds to an energy of $\sim 2.7 \times 10^{-16}$ J for a S/N of 20, with integration times of 5 h, 0.5 h and 15 min, for the required spectral resolutions of $R = 10000$, 1000 and 500, respectively. These estimates assume that there are no losses in the optics or on the detector. The exposure times will be increased once the instrument throughput and detector quantum efficiency is taken into account (see below in this section). With such exposure times, we ensure that a large fraction of galaxies will be studied within a reasonable lifetime for a mission like SUGAR-1 of ~ 5 years. Hence, we take 3.5 meters as the fiducial value for the main mirror diameter of the telescope.

The 3.5 m mirror will be mounted in an Ritchey-Chrétien configuration (see Fig. 5). The other main telescope parameters are listed in Table 2. Graphite fiber materials are needed to reduce the weight of the large mirror. The Al/MgF₂ coating and active optics system will ensure that the losses on the mirror surface are reduced to a minimum, maximizing in this way the throughput of the telescope.


Fig. 5. Sketch of the spacecraft configuration.

On the Cassegrain focus of the telescope, we plan to mount an instrument box containing the optical elements of the spectrograph and the detector (see Fig. 6). Imaging and spectroscopy with SUGAR-1 will be diffraction limited, which is 0'034 for a 3.5 m telescope at a fiducial wavelength of 2500 Å. Given the pixel size of 10 μ m in the detector (see Table 3) and the focal length of the telescope (70 m), the Airy spot will be undersampled in the entrance focal plane of the telescope. We therefore need to use a collimator and camera combination with a magnification factor of 2, to spread the core of Point Spread Function (PSF) in two pixels on the detector plane. The main specifications of the spectrograph as well as the detector are defined in Table 3.

The light arriving at the entrance focal plane passes through a slit. We have chosen a slit width of 0'034, so that the whole PSF is located within the slit, but other slit sizes will be available in the slit wheel. The light is then collimated and sent to a filter wheel that will have at least 6 filters for imaging and one open position for spectroscopy. No blocking filter is needed for spectroscopy because the free spectral range is larger than the wavelength range of interest.

The collimated beam reaches a grating wheel that can be moved about two axes. This allows selecting a diffraction grating as well as tuning the inclination of the grating in order to send the blazed beam towards the detector plane. The grating wheel will have 8 gratings at $R = 10000$ to cover the whole spectral range at intervals of ~ 300 Å, since the Ly α absorption can appear at any wavelength depending on the redshift ($z = 0.4 - 1.1$). Two gratings at $R = 1000$, one grating at $R = 500$ and one flat mirror for imaging. We have calculated the grating specifications for the 3 spectral resolutions (see Table 4), using a slit width of 0'034 and the optical parameters for the camera and collimator listed in Table 3. We plan to use blazed gratings covered with an Al coating and protected with an overcoating of MgF₂.

The light dispersed by the grating (or reflected on the flat mirror) is sent to a camera, and then reflected on a flat tilt mirror before reaching the detector plane. This tilt mirror can rotate around two axes to produce slight variations in the position of the spectrum (or image) on the detector plane.

The detector geometry that we propose is an *inverted T* consisting of a central 2K \times 2K pixels central region and two *side wings* of 1K \times 1K pixels (see Fig. 7). In imaging mode, we will use the central square of 2K \times 2K pixels with a resolution of 2 pixels to sample the PSF, assumed to be 0'034 and a pixel

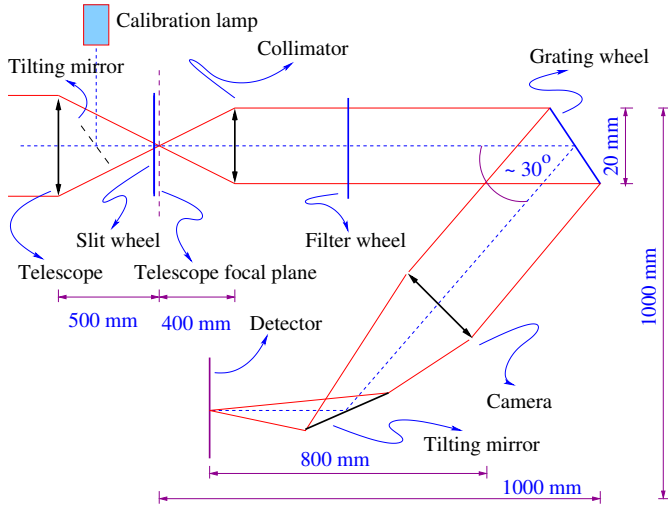


Fig. 6. Spectrograph sketch where the main components and dimensions are represented. The relative dimensions are not to scale.

Table 3. Spectrograph and detector specifications.

Spectrograph	
Approx. dim.	1500×1000×1000 mm ³
Spectral range	1000 Å – 3500 Å
W ^a	0′.034×10″
f _{col}	40 mm
Θ _{col}	20 mm
Filters	8 units (20 mm diam.)
Gratings (R=10000)	8 units (~20 mm diam.)
Gratings (R=1000)	2 units (~20 mm diam.)
Gratings (R=500)	1 units (~20 mm diam.)
f _{cam}	80 mm
Θ _{cam}	~20 mm
Throughput	~50%
Detector	
Det. size ^b	4K×2K pixels
Pix. size	0.01 mm
QE	~50%
Pix. esc. detector	0′.015 pix ⁻¹
Cooling system	Passively cooled
Data handling	
Timing generator	Imaging & CCDs
Acquisitions	Controls detector readout & analogue to digital conversion
Control unit	Images & spectra saved in a resident memory & transmitted to main S/C BUS

W is the physical size of the slit used for the calculations.

f_{col} is the focal length of the collimator.

Θ_{col} is the diameter of the collimated beam.

f_{cam} is the focal length of the camera.

Θ_{cam} is the diameter of the camera beam.

^a Slit size used to perform the calculations yielding the grating parameters of Table 4.

^b See Fig. 7 for the detector geometry.

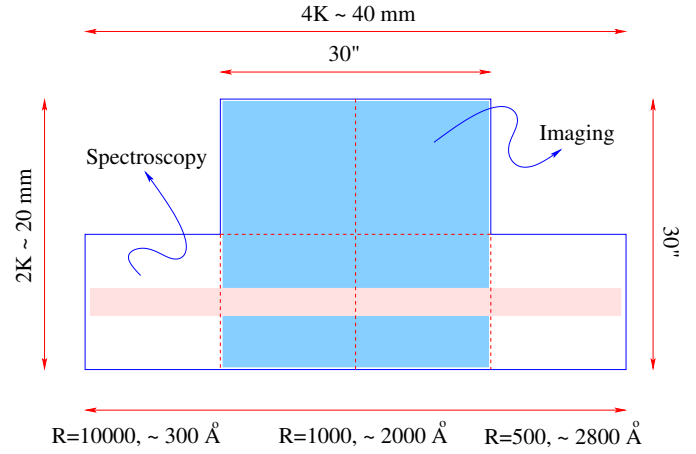


Fig. 7. Detector sketch. Note that the central squared area (2K×2K pixels) is thought to be used for imaging, and the long rectangular area (4K×1K pixels) for spectroscopy.

Table 4. Diffraction grating specifications for blazed incidence in the first order of interference.

Sp. Res.	G (grooves/mm)	θ _B (degg)	α (degg)	β (degg)	L (cm)	P (Å/mm)
10000	3500	37.2	43.4	-8.8	2.7	3.53
1000	350	2.4	13.7	8.8	2.1	35.3
500	170	1.2	27.8	25.4	2.3	70.6

θ_B is the blaze angle.

α is the incidence angle (with respect to the normal to the grating).

β is the diffraction angle.

L is the size of the grating.

P is the plate scale in the spectral direction.

size of 10 μm. In the spectral mode, the detector surface will be a rectangle of 4K×1K pixels, used with a spectral sampling of 0.035, 0.35 and 0.71 Å/pixel for R = 10000, 1000 and 500, respectively.

The two main technologies currently used for UV detectors are coated CCDs and Micro-channel Plates (MCPs). CCDs are limited in UV wavelength coverage but have good quantum efficiency (QE). MCPs have a poor QE but would almost cover our wavelength range. However, this would require two detectors, one for the far UV and the other one for near UV. Therefore, we require some advance in current detector technologies to find a good trade-off between wavelength coverage and quantum efficiency. According to Naletto et al. (1995), we may expect good improvement on the CCD coating technology in the near future.

Hence, we may define our CCD with a quantum efficiency of 50% between 1000 Å and 3500 Å. The exposure times estimated above must be then recalculated also considering that on the light path there are 4 reflections (on mirrors and gratings) and 3 transmissions (through the collimator, filter (imaging only) and the camera lens). Thus, for spectroscopy and wavelengths above 2000 Å, the system has an optics efficiency of 0.59, and for wavelengths below 2000 Å the efficiency is 0.23. For imaging, the efficiency is 0.31. With all this in mind, the exposure time for the spectrometry at R = 10000 with a S/R = 20 becomes 18 h.

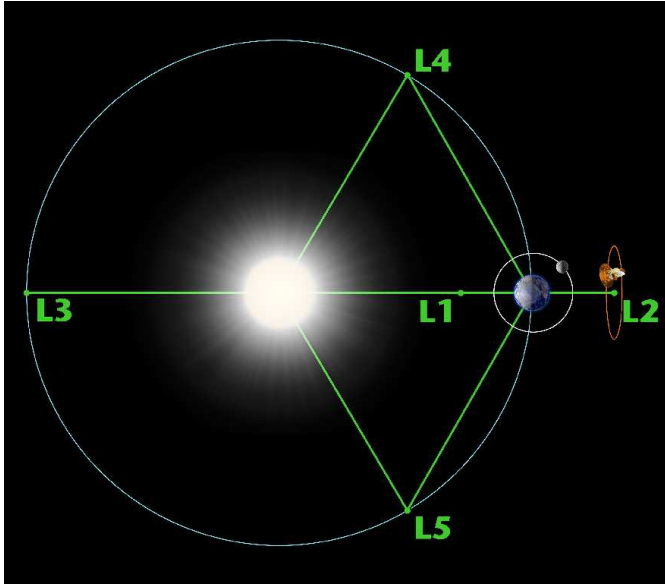


Fig. 8. Representation of the five Lagrangian points (L_1 to L_5) of the Sun-Earth system. At these points, the centrifugal and gravitational force on a third body neutralize each other. The L_1 , L_2 and L_3 points are quasi-stable because they are saddle points in the gravitational field, while L_4 and L_5 correspond to maxima, and hence are points of unstable equilibrium.

6. Mission configuration

We plan to send the aircraft to the L_2 point (see Fig. 8). We have chosen this point because it is easy to reach (1.5 million km from Earth) and only small orbit corrections are necessary to hold the spacecraft in it. The orbit of the L_2 point around the Sun is synchronous with that of the Earth, i.e. for a satellite in L_2 , the Earth is the whole time located between the spacecraft and the Sun. This allows using a relatively elementary thermal control system due to the thermal and radiation stability in this orbit compared to the typical fluctuations in an Earth-orbit.

The structural sub-system of the spacecraft will support the instrumentation during its motion and will also support a cover protecting the internal components against adverse environmental factors. Due to the low forces in the L_2 orbit, we choose to use the cost-effective aluminium structure rather than expensive carbon fibre, which is a lighter and stiffer material option. The spacecraft payload and service module configurations are shown in Table 5.

Energy will be supplied to the spacecraft via solar arrays. The area of the array depends on the general energy consumption of the spacecraft, degradation and predicted end-of-life minimum average efficiency. Telecommunications for a detector size of $4K \times 1K$ pixels will result in 8 Mb of data per image or spectra (see Table 5). This size though, could be appreciably reduced (by a factor of 5 - 10) with loss-less compression algorithms, which would also mean a reduction in the total download time to the ground. A schematic of the electronics of the payload is shown in Fig. 9. The whole process is planned to be under the control of a micro-controller unit.

As it was shown in Section 5, the spectrograph will include a tilting mirror to insert the calibration lamp on the light path,

Table 5. Mission configuration.

Spacecraft	
Dimensions	9m length, 3.7m diam.
Propulsion	Hydrazine (4-5kg /yr)
Orbit	L_2
Pointing ops.	3 axis stabiliz. Pointing error $< 0'.1$
Structure	Al shield (1cm thick, 7m long) Al honeycomb-solar panels Ti - thermal
Payload Module	
Optics	Volume 53.4 m ³
Telescope config.	Ritchey-Chrétien
Telecommunications	
Data	8 Mb per image/spectra
Down-link freq.	~ 8 GHz
Up-link freq.	~ 2 GHz
S/C antenna	~ 1.3 m diameter
Transmitter output	5 W
Power supply - Solar arrays	
Cells	Ultra Triple Junction
BOL min effic.	$\sim 28.3\%$
Cell struct.	Layered GaInP ₂ /GaAs/Ge
Lifetime	~ 5 yr nominal ~ 7 yr extended
Launcher	Ariane 5 ES
Power consumption	
Telescope	10 W
Communication	50 W
Detectors & electronics	40 W
Orbit/pointing control	77 W

a slit wheel, a filter wheel and a grating wheel. For the three wheels, we will use classical technology like stepper motors and/or torque motors, which allow the rotation of the platform containing the optical elements. For tilting mirrors an interesting alternative is the development of a Micro-Opto-Electro-Mechanical device (MOEM). The main advantage of MOEMs is the possibility to place the optical elements in the system with the ability for precise and controlled motion. The main problem is the very small size of the optical elements. Also the reliability still needs to be investigated.

To ensure the success of the mission, tests will have to be performed on different elements of the spacecraft, including a complete proto-flight model (PFM). A list of the most important elements of the mission that should be tested and the type of tests that should be performed is,

- *Structure.* Vibrational, thermal.
- *Mirrors.* Vibrational, acoustic, thermal, optical.
- *Instrument.* Vibrational, thermal, optical, electrical.
- *Mechanical.* Grating wheels, gyroscopes.
- *Telecommunications antenna.* Vibrational, deployment, data transfer.
- *Solar panels.* Vibrational, thermal, functional deployment.
- *Whole S/C.* Thermal, vibration, electrical, functional.

We propose a nominal mission lifetime of ~ 5 years, which will allow finishing the SUGAR-1 survey within the constraints

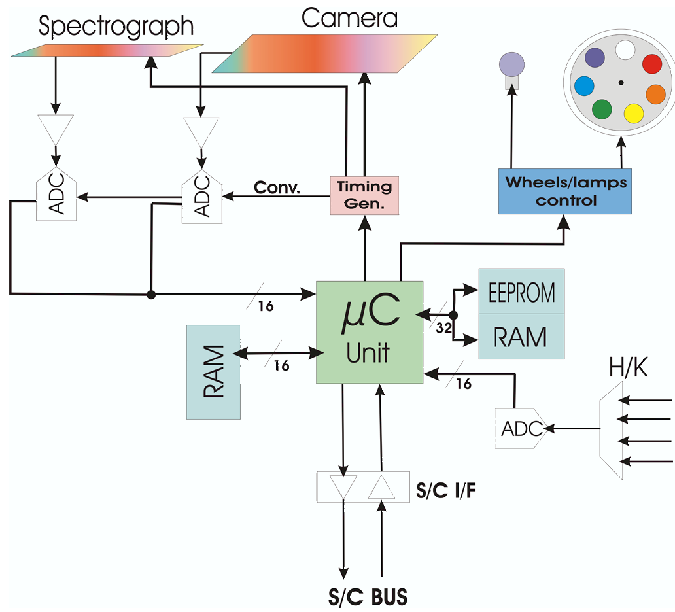


Fig. 9. Sketch of the electronic system.

Table 6. Mass considerations.

Mass		kg
Communications	Solar Baffle	40
	Space Antenna	14
	Transmitter	4
Optics	Primary Mirror	48
	Secondary Mirror	1
	Primary Actuators	83
	Secondary Actuators	1
	Primary Mirror Support	92
	Metering Truss	7
Instruments	Science	10
	Elec. power	52
	Thermal Control	5
	On-board Computer	1
	Attitude Control	47
Base	Fuel, Tank, Thrusters	140
	Spacecraft structure	588
Total Mass		1133

given by the long exposure times needed for the sensitive spectroscopic observations. However, we forecast an extended mission lifetime of 7 years. Once the nominal mission is concluded, the extension would depend on the interest and funds available at that time.

7. Mass and cost budgets

The mission requires a budget of approximately 400 million euros based on the Satellite Design Tool Spreadsheet provided on the Albach Shared Server (see Table 7). These costs were estimated for an unmanned spacecraft launched with Ariane. To help reduce launch costs, we can consider launching with the Soyuz Fregat, which would require a deployable telescope structure. Alternatively it might be possible to launch SUGAR-1 as part of a larger mission.

Table 7. Costs in million euros.

Space	Spacecraft: 69–175
Launch	Ariane: 150
	Insurance: 50

8. Summary

We have presented a medium cost (400 million euros) mission consisting of a 3.5 m UV telescope, which feeds a spectrograph and imager at the spatial diffraction limit, with spectral resolutions from low ($R = 500$) to relatively high ($R = 10000$). Such a mission will cover an existing gap in the UV spectral range in the near-future plans of ESA and NASA.

We suggest the utilization of this UV space telescope to solve major science questions of cosmological implications related to the star formation history of the Universe at a redshift $z \sim 1$, which corresponds to an epoch of enhanced star formation rate density, and to the time when our Solar System was formed. Such a mission, named SUGAR-1 (Spectrometry in Ultraviolet of GALaxies at Redshift-1), is thought as a long-term survey of candidate galaxies at redshift $z \sim 1$, extracted from ground-based databases (e.g. the Sloan Digital Sky Survey).

What has been presented here is the result of two weeks of intense and exciting work in the frame of the 28th Albach Summer School. We consider the participation in the school definitely a wonderful experience. We have not only learned more about many topics related with space science but what is more important, we have learned to work as a team in an international environment to achieve a specific goal in a limited amount of time. We think this will be very useful in our future careers, since this is a very good approximation to how space projects are defined nowadays.

Acknowledgements. We would like to thank ASA and ESA for having given us the opportunity of participating in the 28th Summer School Albach. Special thanks to all the tutors and lecturers for their patience and invaluable help in preparing this work. Thanks to all funding organisms and institutions that have contributed to fund partially or totally the costs for the participation in the School.

References

- Cerviño, M. & Mas-Hesse, J. M. 1994, A&A, 284, 749
- Heckman, T. M., Sembach, K. R., Meurer, G. R. et al. 2001, ApJ, 558, 56
- Leitherer, C., Schaerer, D., Goldader, J. D. et al. 1999, ApJS, 123, 3
- Lilly, S. J., Le Fevre, O., Hammer, F. et al. 1996, ApJL, 460, 1
- Madau, P., Ferguson, H. C., Dickinson et al. 1996, MNRAS, 283, 1388
- Madau, P., Pozzetti, L. & Dickinson, M. 1998, ApJ, 498, 106
- Mas-Hesse, J. M. & Kunth, D. 1991, A&AS, 88, 399
- Naletto, G., Pace, E., Placentino, L. et al. 1995, SPIE, 2519, 31
- Rosa-González, D., Terlevich, E. & Terlevich, R. 2002, MNRAS, 332, 283